Journal of Marine Science and Technology
https://doi.org/10.1007/s00773-023-00967-0

ORIGINAL ARTICLE

Reliability assessment of the ocean thermal energy conversion systems through Monte Carlo simulation considering outside temperature variation

Amir Ghaedi[1] · Reza Sedaghati[2] · Mehrdad Mahmoudian[3] · Eduardo M. G. Rodrigues[4,5] · Radu Godina[6,7]

Received: 14 May 2023 / Accepted: 19 October 2023

Abstract
The ocean thermal energy conversion (OTEC) systems, as renewable energy-based power plants, have the potential to play a significant role in meeting future electricity demands due to the vast expanse of the world's oceans. These systems employ the temperature difference between surface ocean waters and deep ocean waters to drive a thermodynamic cycle and produce electricity. The temperature of deep ocean waters, approximately 1000 m below the surface, is approximately 4 °C, while surface ocean temperatures typically range between 20 and 30 °C. The generated power of OTEC systems is dependent on these temperature differences and may vary with changes in surface ocean temperatures. In this study, the main focus is to find the impact of temperature variation on the failure rates of OTEC system components and the generated power output of these plants. The findings indicate that as the demand for the power system increases, its reliability decreases. In order to improve the reliability of the power system, the integration of a new generation unit, such as the close cycle OTEC power plant under investigation, could be necessary. The findings also indicate the importance of considering temperature variation in the evaluation of the reliability of such types of power plants based on renewable energy.

Keywords Reliability · Ocean thermal energy conversion system · Temperature variation · Failure rate · Monte Carlo simulation · Markov models

✉ Radu Godina
r.godina@fct.unl.pt

Reza Sedaghati
sedaghati.r@biau.ac.ir

[1] Department of Electrical Engineering, Dariun Branch, Islamic Azad University, Dariun, Iran

[2] Department of Electrical Engineering, Beyza Branch, Islamic Azad University, Beyza, Iran

[3] Department of Electrical and Electronic Engineering, Shiraz University of Technology, Shiraz, Iran

[4] INESC-ID, Sustainable Power Systems Group, Av. Rovisco Pais 1, 1049-001 Lisbon, Portugal

[5] Instituto Superior Técnico, University of Lisbon, Av. Rovisco Pais 1, 1049-001 Lisbon, Portugal

[6] Research and Development Unit in Mechanical and Industrial Engineering (UNIDEMI), Department of Mechanical and Industrial Engineering, NOVA School of Science and Technology, Universidade NOVA de Lisboa, 2829-516 Caparica, Portugal

[7] Laboratório Associado de Sistemas Inteligentes, LASI, 4800-058 Guimarães, Portugal

1 Introduction

Given that the oceans account for more than 70% of the Earth's surface, oceanic energy sources such as wave, tidal, and thermal energy have the potential to generate a significant proportion of the required electricity [1]. The temperatures of surface seawater in the ocean typically range from 20 to 30 °C [2], while the temperatures of ocean waters at a depth of 1000 m are approximately 4 °C. These temperature differences can be leveraged to drive a thermodynamic cycle, utilizing surface seawater as a warm source and deep seawater as a cold sink, in order to derive a working fluid such as ammonia and generate electricity [3, 4]. The conversion of oceanic energy into electricity through the utilization of the temperature differential between warm and cold seawaters has led to the development of three types of ocean thermal energy conversion (OTEC) systems: open cycle, close cycle, and hybrid OTEC power plants [5]. In the realm of OTEC systems, the open cycle configuration employs ocean water as its working fluid. In this system, surface ocean water is pumped into a flash evaporator, where the pressure of 0.03

Published online: 06 November 2023

bars causes it to boil at a temperature of 22 °C. The generated vapor drives a turbine, which in turn powers a generator. The vapor then condenses into desalinated water through the transfer of heat to deep seawater in a condenser. On the other hand, the close cycle OTEC power plant utilizes surface ocean water as the warm source to vaporize a low boiling point working fluid, such as ammonia, into vapor [6]. The generated vapor is directed into a turbine where electricity is produced. Subsequently, the vapor is passed through a heat exchanger where it condenses using deep seawater that has been pumped into the condenser. The hybrid OTEC power plant combines the benefits of both the open and closed cycle systems [7]. In general, the implementation of OTEC systems is associated with substantial costs due to the requirement of substantial infrastructure as well as the limited thermal efficiency of the system. The substantial capital expenditures required to build the necessary infrastructure and the limited efficiency of the system make OTEC systems cost-prohibitive for many applications [8].

The output power of OTEC power plants is influenced by the temperature of cold and warm seawater. While the temperature of seawater at the ocean's surface fluctuates over time, the power generation capacity of the plant can vary and therefore impact its reliability. Previous studies have explored the reliability of OTEC power plants, and insights can also be gained from studies of other variable output renewable energy sources such as solar (in which photovoltaic failures are studied) [9], wind, tidal, run-of-the-river, and wave, which are influenced by variations in water flow rate, solar radiation, wind speed, tidal height and current speed, and wave height and period [10, 11]. In previous studies [10, 11], both long-term and short-term evaluations of the reliability of power systems incorporating an OTEC power plant have been conducted. In [11], a multi-state reliability model is developed for OTEC power plants, considering both fluctuations in the generated power and component failures. Key elements of a close cycle OTEC power plant are analyzed, including the principal structure, mooring system, pipes, turbine, generator, evaporator, condenser, pumps, control system, transformer, and cable, are considered, and their impact on the overall failure of the plant. Also in [11], the fuzzy c-means clustering method is employed to reduce the number of states in the reliability model, with the optimal number of clusters being determined using the Xie and Beni index. In reference [10], the spinning reserve required for a power system incorporating large-scale OTEC power plants is determined using a modified PJM method. This paper presents a multi-state reliability model that is suitable for short-term studies of the power system and is specifically designed for OTEC systems. The proposed reliability model takes into account the failure rate of the primary components and the variation in the generated power of the plant due to changes in the temperature of the ocean surface water. It should be noted that the repair rate has not been taken into consideration in this model. The reliability performance of other ocean energy-based generation units, such as barrage type tidal power plants [12, 13], current type tidal power plants [14], and wave energy conversion [15] devices based on the sea wave slot coned generator technology, are researched. In [13, 16], a large-scale barrage type tidal power plants is analyzed and a multi-state reliability model is proposed that considers both the failures of the constituent components and the fluctuations in the generated power resulting from variations in tidal height. In [13], the long-term adequacy of the power system incorporating a barrage type tidal power plant is assessed, while [16] focuses on operational studies of the power system to find out the necessary spinning reserve while taking into account the impact of the barrage type tidal power plant. In [14], a multi-state reliability model is designed for the current type tidal turbines to be utilized in the assessment of the power system's adequacy. The generated power of these turbines can vary over time due to variations in tidal current speed, and the fuzzy c-means clustering technique is employed to minimize the states' number in the reliability model. In reference [17], the effect of fluctuations in wave height and wave period on the reliability modeling of wave energy conversion systems that utilize the sea wave slot coned generator technology is investigated. The generation capability of the wave converters is contingent on wave height and wave period. As a result, due to fluctuations in these parameters, the power output of the wave converters changes over time, impacting their reliability.

In several studies the authors explore the reliability models and methods for assessing the impact of renewable energy on the availability of power generation [18–23]. These models offer insight into the effect of integrating distributed generation, particularly from renewable sources, on the reliability of distribution systems. The studies delve into the unique characteristics of reliability models for wind, small hydro, solar, run-of-the-river, and biomass energy, and examine the methods used to evaluate their reliability when integrated into distribution systems. Whether through analytical techniques, Monte Carlo simulation, or a hybrid approach, these methods shed light on how distributed generation affects the reliability of the system. Yet, the greatest uncertainty arises from intermittent renewable energy sources, where both the availability of the energy source and the generating unit determine the availability of power generation. In the reviewed literature, the effect of fluctuation in wind speed, solar radiation, and water flow rate on the generation output and subsequent reliability of renewable energy-based power plants has been investigated. However, the effect of temperature variation of the air and seawater, tidal height, tidal current speed, wave height and period, wind speed, solar radiation, and water flow rate on the failure

rate of the elements constituting these power plants has not been thoroughly studied in previous works.

In the previous research performed on the reliability of OTEC power plants, the failure rate of its comprised components is considered to be constant. A multi-state reliability model, proposed in [11], that is obtained from hourly seawater temperature data can be applied for long-term reliability evaluation of power systems containing OTEC plant, regardless of failure rate changes. In these studies, seasonal seawater temperature data can be used to determine the multi-state reliability model of the OTEC plant with less precision. However, the innovation of the current study is that it takes into account the effect of changes in seawater and air temperature on the equipment failure rate, and for this reason, this study has a much higher precision.

In several studies the influence of the variations in wind speed, tidal height, and tidal current speed on the failure rates of the components of wind energy generation units, barrage type tidal power plants, and current type tidal turbines are examined [12, 24–26]. These studies also investigate the effect of fluctuations in renewable resources on the failure rates of the back-to-back converters employed in tidal and wind turbines, as well as the failure rates of the turbine, transformer, generator, and cable.

In this study, the effect of seawater and air temperature variations on the reliability of OTEC power plants is analyzed. The change in the failure rates of the elements of the OTEC power plant, including the pumps, generator, transformer, electrical converter, turbine, and cable, is taken into account. This consideration is crucial for the reliability evaluation of power systems that include OTEC power plants. The current paper seeks to examine the impact of seawater and air temperature variations on the reliability performance of OTEC power plants. In the second section, the components of OTEC power plants and the equations for determining their generated power are presented. The impact of seawater and air temperature on the failure rates of these components is discussed in the third section. The fourth section proposes a Monte Carlo simulation-based technique to evaluate the adequacy of power systems that incorporate OTEC power plants, taking into account the variable failure rates of the components. Numerical results and the conclusion are provided in the fifth and sixth sections, respectively.

2 Failure rate analysis methodology

In the past, a significant amount of research has been conducted regarding the equipment failure rate in electric power distribution networks. This research has encompassed a range of concepts, estimation techniques, and modeling methodologies aimed at understanding the behavior and performance of the equipment in these networks. By examining the various factors that contribute to equipment failure, researchers have sought to identify strategies for reducing equipment failure rates and improving the overall reliability of these critical infrastructure systems [27].

In recent years, the field of power system reliability modeling and computation has experienced significant advancements due to the application of probability theory [28]. This is a crucial area of study as failures in power systems can result in significant consequences [29]. The analysis of reliability is essential in minimizing system downtime and reducing the frequency of failures, making it a critical topic in the field of electrical power systems. The advancement of quantitative analysis has provided a means of improving reliability and reducing the negative impact of failures in power systems [30].

In risk analysis, the estimation of failure rate is a significant source of uncertainty, particularly in determining the frequency of failures in any given equipment. The concept of failure rate is complex and encompasses various aspects of equipment operation that are susceptible to external factors that can negatively impact its performance and cause a failure. To effectively reduce risk, it is imperative to consider the failure rate parameter through the use of appropriate quantification tools. This will enable a more accurate assessment of the risk associated with equipment operation [31].

2.1 Monte Carlo simulation

Monte Carlo simulation is a widely utilized method for predicting the behavior of a system over time. This approach leverages the concept of simulating all possible outcomes based on the decisions made, providing researchers with a comprehensive evaluation of the risk and its impact [32]. The technique of Monte Carlo simulation is highly advantageous in managing risks within an organization, as it enables researchers to visualize the results of their decisions [33].

The Monte Carlo simulation method is a statistical technique that uses repeated random sampling to model and analyze the impact of uncertainty in a system. This approach is grounded in the principle of building models that represent potential outcomes by assigning random values or probability distributions to uncertain variables. By running the simulation multiple times with a diverse sets of random values, a recalculation of the result occurs [34]. The number of required recalculations depends on the number of uncertain factors and the ranges specified. Depending on the level of uncertainty and the ranges defined, the simulation may require thousands or even tens of thousands of iterations [35].

2.2 Markov modeling for reliability

Markov models are mathematical models that describe processes that satisfy the Markov property, which refers to systems that can be described as existing in one of a number of possible discrete states at any given time. These models are based on the concept of state transitions, where the likelihood of transitioning from a certain state to a different state determines the behavior of the system. Unlike other models, Markov models do not take into account the preceding history or states' sequence that took place before the current state, but only consider the current state and the probability of transitioning to other states [36]. This makes them a useful tool for analyzing systems that exhibit this type of behavior, as they provide a simplified representation that captures the essential features of the underlying process.

The modeling of complex repairable systems works well with stochastic techniques [37]. The Markov model for systems that can be repaired is a mathematical tool that is utilized to analyze the behavior and reliability of systems in which the components' repair is performed in response to a failure event, rather than as a preventive or corrective maintenance measure. This model considers the probability of transition between different states of a system, rather than its history or sequence of previous states, to assess the performance and reliability of the system's components. The repairable system's Markov model differs from traditional maintenance models, as repairs are only conducted when individual components fail, and not when the entire system is out of operation [38].

The Markov model is a widely used tool for finding out the systems' reliability in several fields of study [39] due to its ability to take into consideration multiple factors that impact system performance. These factors may include redundancy, periodic testing, fault-tolerance, fault coverage, and different failure modes. In order to effectively apply the Markov model for reliability evaluation, it is essential to first identify the elements of the equipment and the distinct operational states it can be in. Once the identification of these states occurs, a fitting Markov model could be developed based on the identified states and used to evaluate the equipment's reliability [32].

3 The close cycle OTEC power plants

Among different types of the OTEC power plants, a close cycle system is installed and operated in Hawaii in August 2015. The generated power of this plant is connected to the power grid. Therefore, in the present study, a reliability model for a closed-cycle OTEC power plant is proposed. One of thermodynamic closed cycles widely used in the closed-cycle OTEC power plant is the Rankine cycle. The structure of a representative closed-cycle OTEC plant based on the Rankine cycle is depicted in Fig. 1.

By closely observing Fig. 1, a close cycle OTEC power plant based on the Rankine cycle is composed of three pumps for pumping the working fluid such as ammonia, deep seawater as the cold sink and seawater placed on the ocean surface as the warm seawater to the thermodynamic cycle, evaporator for converting the ammonia to the vapor, condenser for converting the vapor to the liquid ammonia, turbine, generator, transformer and cable. The other important components of a close cycle OTEC plant not presented in the figure are the main structure of the plant, mooring system and different pipes for transmitting the ocean waters to the thermodynamic cycle. The thermodynamic cycle utilized in close cycle OTEC power plants is based on the Rankine cycle [40], with ammonia commonly employed as the working fluid. The seawater placed on the ocean surface is pumped into the evaporator, which is a heat exchanger that contains the high pressure liquid ammonia. Thus, the heat of the warm seawater is transferred to the ammonia and the ammonia is converted into the vapor. The obtained ammonia vapor is entered into the turbine and produces the electricity using the rotation of the generator and the turbine linked to the turbine. Then, the ammonia vapor is entered into the condenser. In addition to the ammonia vapor, the deep seawater is pumped into the condenser and results the ammonia vapor condenses. Then, the liquid ammonia is pumped into the evaporator and the Rankine cycle is completed.

The temperature-entropy and pressure-enthalpy diagrams of the Rankine cycle utilized in the close-cycle OTEC power plant are depicted in Figs. 2 and 3. This thermodynamic cycle serves as the basis for calculating the generated power of the close-cycle OTEC power plant, as represented by the following equation:

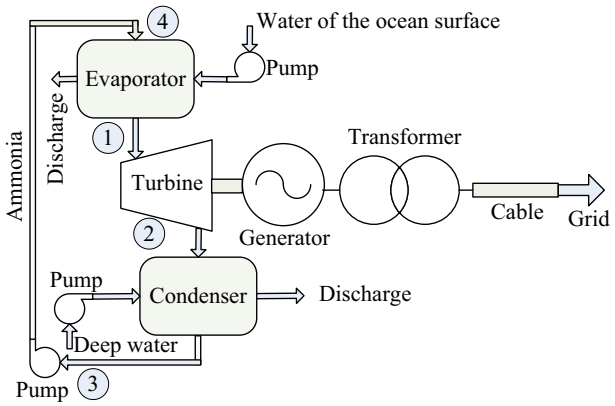

Fig. 1 The structure of an OTEC power plant based on the Rankine cycle

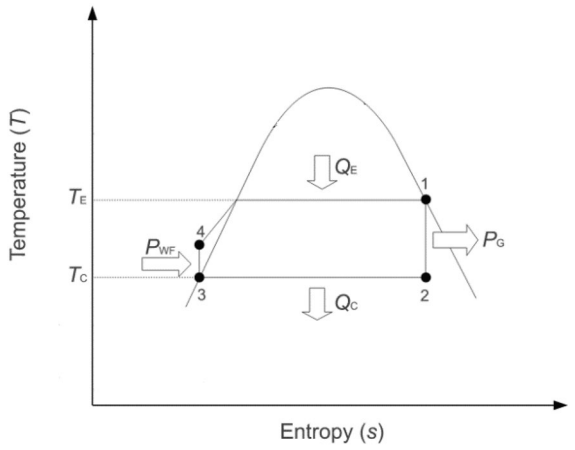

Fig. 2 The temperature of the Rankine cycle versus the entropy in the close cycle OTEC power plant

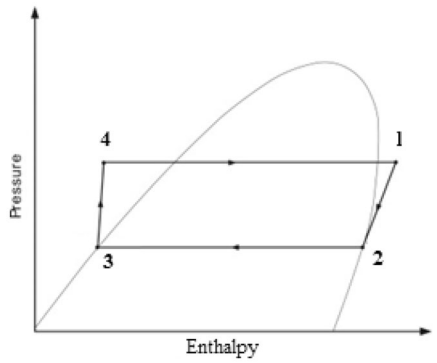

Fig. 3 The pressure of the Rankine cycle versus the enthalpy in the close cycle OTEC power plant [41]

$$P_{tur} = \dot{m}\eta_t\eta_g(h_1 - h_2) \tag{1}$$

where P_{tur}, $\dot{m}$, η_t, η_g, h_1 and h_2 are the output power of the plant, the mass flow rate of the working fluid, the turbine efficiency, the generator efficiency, the enthalpy of the evaporator outlet that is the same as the turbine inlet and the enthalpy of the turbine outlet that is the same as the condenser inlet.

To determine the h_1 and h_2 in the Rankine cycle, it can be used from the thermodynamic table of the working fluid. The thermodynamic properties including pressure, specific volume, entropy and enthalpy of the ammonia usually used in the close cycle OTEC power plant for different temperatures are presented in [42–44]. In the closed-cycle OTEC power plant, the temperature of the seawater at the ocean surface is taken as the temperature of the saturated vapor of ammonia at state 1, while the temperature of deep seawater is considered as the temperature of the saturated liquid of ammonia at state 3. According to the temperatures of the ocean surface and deep seawaters, the pressure, enthalpy and entropy of the states 1 and 3, i.e. the saturated vapor and liquid of ammonia are determined using the thermodynamic table of the ammonia. As mentioned, in the Rankine cycle of the close cycle OTEC plant, the states 1 and 3 are considered to be the saturated vapor and saturated liquid of ammonia. Thus, the following equations can be written for the understudied Rankine cycle:

$$\begin{aligned} &h_3 = h_f,\ s_3 = s_f,\ v_3 = v_f,\ p_3 = p_2 \\ &p_1 = p_4,\ h_1 = h_g,\ s_1 = s_g \end{aligned}, \tag{2}$$

where *h, s, v* and *p,* are the enthalpy, entropy, specific volume and pressure of the working fluid in different states. In the closed-cycle OTEC power plant, the temperature of the ocean surface water is considered to be the temperature of the ammonia-saturated vapor in State 1, while the temperature of the deep seawater is considered to be the temperature of the ammonia-saturated liquid in State 3. The States 1 to 4 are associated with the saturated vapor at the turbine inlet or evaporator outlet, the turbine outlet or condenser inlet, the condenser outlet or pump inlet, and the pump outlet or evaporator inlet, respectively. As seen in the temperature-entropy diagram of the Rankine cycle used in the closed-cycle OTEC power plant, State 2 is a mixture of the saturated liquid and saturated vapor of the ammonia. In Eq. 2, the quality of the mixture is defined as the ratio of the vapor mass to the total mass and is represented by the symbols “f” and “g” for the saturated liquid and saturated vapor states, respectively. In the close cycle OTEC power plant, the turbine expansion process would be isentropic. The isentropic process is a specific type of adiabatic process, where there is no transfer of matter or heat. In this process, the gas or fluid has constant entropy. Thus, in the constant-entropy process, the system is taking turbine power:

$$s_1 = s_2. \tag{3}$$

To determine the quality of state 2, the entropy of state 2 is available and Eq. 4 can be used for this purpose:

$$x = \frac{s_2 - s_f}{s_{fg}} = \frac{s_1 - s_3}{s_{fg}}, \tag{4}$$

In 4, the symbol “fg” refers to vaporization that is a phase transition from the liquid phase to vapor. Therefore, the enthalpy of state 2, necessary for assessing the plant’s generated power, can be determined as the following equation:

$$h_2 = h_f + xh_{fg} = h_3 + xh_{fg}. \tag{5}$$

To determine the net power of OTEC power plant, the power consumption of the pumps must be deducted from the production power of the turbine.

$$P_{net} = P_{tur} - P_{wfp} - P_{wwp} - P_{cwp}, \tag{6}$$

where P_{wfp}, P_{wwp} and P_{cwp} are the consumed power of working fluid pump, warm seawater pump and cold seawater pump, respectively. P_{net} is the net power of OTEC plant. The power consumption of the pumps can be determined as:

$$P_{wfp} = \frac{\dot{m}_{wf}(h_4 - h_3)}{\eta_{wfp}} \tag{7}$$

$$P_{wwp} = \frac{\dot{m}_{ww} g h_{ww}}{\eta_{wwp}} \tag{8}$$

$$P_{cwp} = \frac{\dot{m}_{cw} g h_{cw}}{\eta_{cwp}} \tag{9}$$

where $\dot{m}_{wf}$, $\dot{m}_{ww}$ and $\dot{m}_{cw}$ are mass flow rate of working fluid, warm seawater and cold seawater, g is the gravitational acceleration, h_{ww} and h_{cw} are the depth of warm and cold seawater, η_{wfp}, η_{wwp} and η_{cwp} are the efficiency of working fluid pump, warm seawater pump and cold seawater pump, respectively.

To accurately determine the generated power of the OTEC plant, the actual temperature of ammonia in evaporator and condenser should be determined. In evaporator, the warm seawater is pumped into this heat exchanger to vaporize the ammonia. The heat equation of this heat exchanger would be:

$$\dot{m}_{wf} q_h = \dot{m}_{ww} q_{ww} \tag{10}$$

In 10, q_h is the heat required for vaporizing the working fluid, and q_{ww} is the heat transferred from the warm seawater to the working fluid. In condenser, the cold seawater is pumped into this heat exchanger to condense the ammonia. The heat equation of this heat exchanger would be:

$$\dot{m}_{wf} q_c = \dot{m}_{cw} q_{cw} \tag{11}$$

In 11, q_c is the heat transferred from ammonia vapor for condensing the working fluid, and q_{cw} is the heat transferred to the cold seawater. The flowchart used in this paper for calculating the hourly generated power of a closed-cycle OTEC power plant equipped to the low-boiling point working fluid such as ammonia is presented in Fig. 4. In this paper, the hourly generated power of the OTEC power plant during a year is determined. Thus, 8760 hourly generated powers would be calculated.

4 The failure rates of the comprised elements of the OTEC power plants

In this section, the effect of the temporal variation of the surface ocean water temperature on the reliability performance of close cycle OTEC power plants is studied. This variation affects the failure rates of key components of these plants, including the pump, transformer, generator, turbine, and cable, as depicted in Fig. 5. However, it is noted that the changes in air and seawater temperature do not significantly impact the failure rates of other equipment within the OTEC power plants, such as the main structure, mooring systems, and pipes.

In this section, a two-state Markov model, as illustrated in Fig. 6, is proposed to evaluate the reliability performance of the various components of the OTEC power plant. In the field of reliability analysis, Markov processes are widely utilized due to their ability to model arbitrary time intervals as Poisson processes. This property allows for the modeling of time to failure and repair as exponential distributions, which is a commonly observed behavior in real-world systems [46]. The probabilities associated with the "up" and "down" states of the model can be assessed by employing the following mathematical expression [47]:

$$A = \frac{\mu}{\lambda + \mu}, \; U = 1 - A \tag{12}$$

where A, U, λ and μ represent the availability or probability of the component being in an "up" state, the unavailability or probability of the component being in a "down" state, the failure rate, and the repair rate, respectively.

4.1 Pumps

In the close cycle OTEC power plants, three pumps including the working fluid pump, the deep seawater pump and the ocean surface water pump are used to rotate the ammonia in the Rankine cycle, to pump the cold seawater to the condenser and to pump the warm seawater to the evaporator, respectively. The impact of temperature variation on the fatigue strength of alloy steels used in pumps is investigated in [48]. Besides, this equation can be applied for determining the failure rate variation of carbon steel. However, carbon steel is not compatible with seawater. In this paper, the warm seawater is pumped from the depth of 1 m. Thus, the warm seawater pump is exposed to the temperature of seawater located at this depth. As a result, the failure rate of the pumps, by taking into account the variation in seawater temperature, can be assessed by employing the following equation:

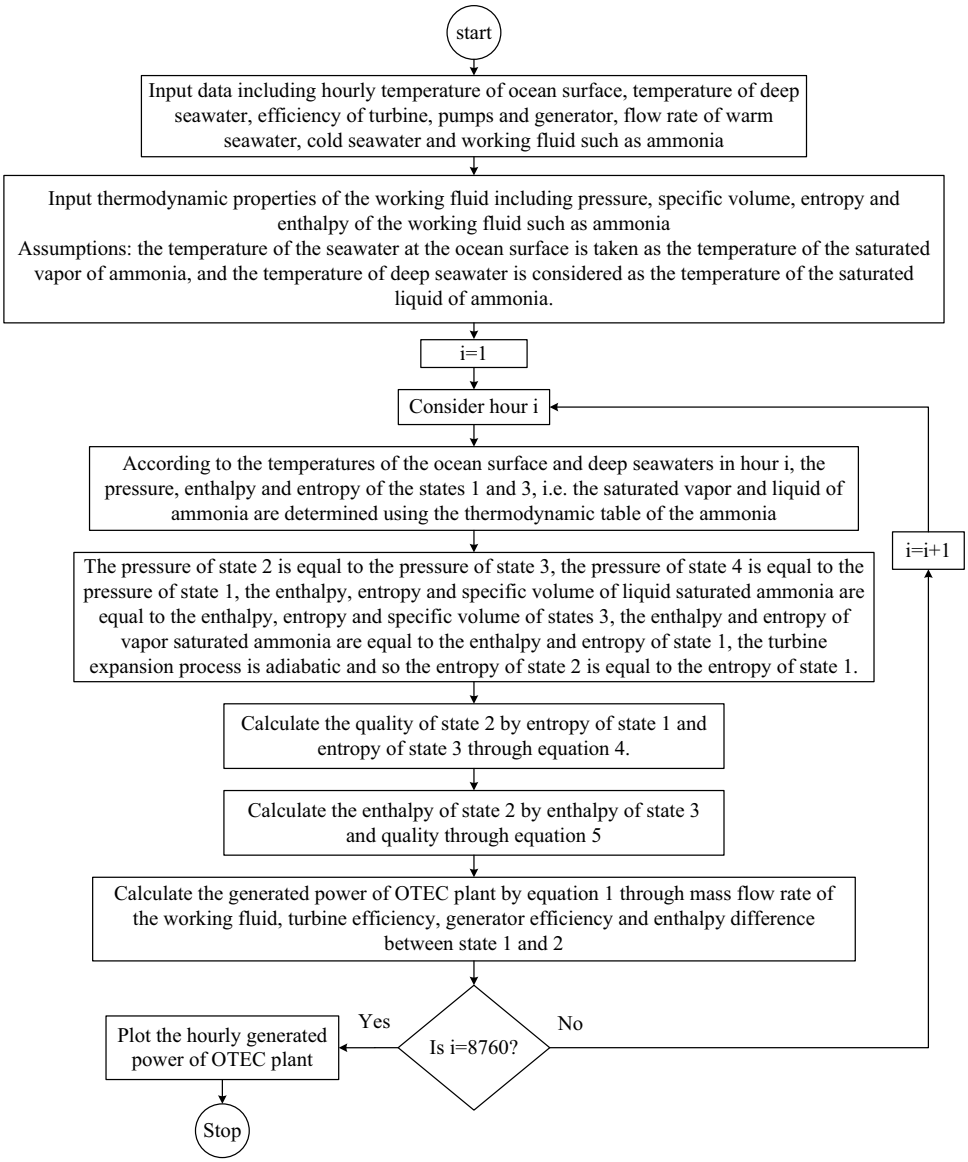

Fig. 4 The flowchart for calculating the generated power of OTEC plant

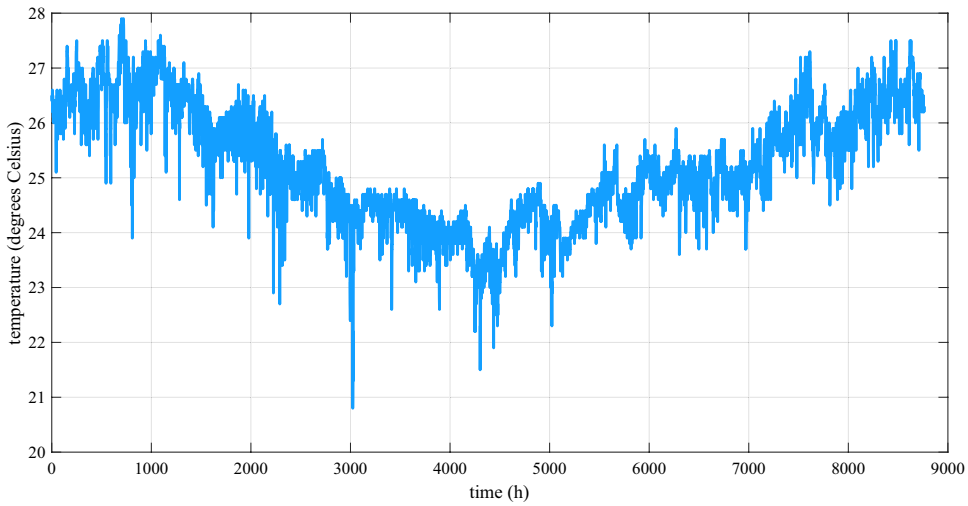

Fig. 5 The hourly temperature of the ocean surface during a year [45]

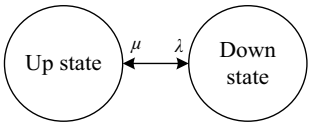

Fig. 6 Illustration of the two-state Markov model for the components

$$\lambda(T) = \lambda_0[0.975 + 0.000432(1.8T + 32) - 0.115 \times 10^{-5}(1.8T + 32)^2 + 0.104 \times 10^{-8}(1.8T + 32)^3 - 0.595 \times 10^{-12}(1.8T + 32)^4] \quad (13)$$

where $\lambda(T)$, λ_0 and T represent the failure rate of the pump at a temperature of T °C, the failure rate of the pump at a temperature of 21.1 °C and the seawater temperature in °C, respectively. Then, the temperatures of the deep seawater pump and working fluid pump are about the temperature of the deep seawater that is considered to be 4 °C. Thus, the failure rates of these two pumps are calculated as 13 by considering the temperature of 4 °C as the operating temperature of the pumps. The operating temperature of the warm seawater pump would be about the temperature of the seawater placed on the ocean surface. As a result of the fluctuations in the temperature of the surface of the ocean, the failure rate of the warm seawater pump is influenced and can be calculated as described in Eq. 13.

4.2 Turbine

The inlet temperature of the ammonia vapor entering the turbine is equivalent to the temperature of the warm seawater pumped into the evaporator. Therefore, the operating temperature of the turbine is equal to the temperature of the water surface in the ocean. The turbines utilized in the OTEC power plants are constructed from carbon and alloy steels and thus, Eq. 13 can be utilized to calculate the failure rate of these turbines. However, due to variations in the temperature of the water surface in the ocean, the failure rate of the turbine changes over time and must be taken into account during the reliability assessment of the OTEC power plants.

4.3 Generator

In the close cycle OTEC power plant, the turbine is connected to the generator for electricity generation. The generators used in the OTEC power plants are based on the permanent magnet synchronous or electrically excited synchronous generators. In the technology utilized in OTEC power plants, the stator voltage is a function of the rotation speed of the generator and the magnetic flux produced by the permanent magnet or the direct current in the field winding. As such, variations in temperature do not significantly impact the generator voltage. However, as per Eq. 1, the generated power of the generator is influenced by the temperature of the ocean surface. Consequently, the current in the stator windings and the power loss of the generator are dependent on the temperature of the ocean surface, which can be determined using the following equation:

$$t_g = t_a + r_{thg}P_{loss} \quad (14)$$

where t_g, t_a, r_{thg} and P_{loss} represent the operating temperature of the generator, the ambient temperature, the thermal resistance of the generator as determined through thermal modeling, and the power loss of the generator, respectively. As can be seen in the 14, the operating temperature of the generator is affected by two variable temperatures, i.e. the ambient temperature is influenced by the air temperature, while the power loss of the generator is influenced by the ocean surface temperature. Therefore, to calculate the failure rate of the generator, the operating temperature of the stator windings is determined as per Eq. 14. The electrical component's failure rate can then be calculated using the Arrhenius law, as detailed in references [49, 50]:

$$\lambda_{eg} = \lambda_{eg0}e^{-\frac{E_a}{k}\left(\frac{1}{t_g+273}-\frac{1}{298}\right)} \quad (15)$$

where λ_{eg}, λ_{eg0}, E_a and k represent the electrical part failure rate of the generator at an operating temperature of t_g, the electrical part failure rate of the generator at a temperature of 25 °C, the activation energy, and the Boltzmann constant, respectively. The relationship between the mechanical part failure rate of the generator and temperature is equivalent to the expression given in Eq. 13. Hence, the overall failure rate of the generator can be assessed by summing the electrical and mechanical part failure rates.

4.4 Transformer

In order to calculate the failure rate of the oil-type transformers used in OTEC power plants, the operating temperature of the transformers must be determined. For this purpose, the operating temperature of the transformers, taking into account the ambient temperature and the winding currents, can be calculated according to IEC 60076-7 [51] through the following equation:

$$t_t = t_a + t_{r0}\left(\frac{1 + r_t r_i}{1 + r_t}\right)^m + ur_r r_i^n \quad (16)$$

The operating temperature of the transformer windings, denoted by t_t, is influenced by a number of factors, including the temperature rise of the transformer associated with

steady-state conditions at rated current (t_{r0}), the ratio of windings losses in the rated current to the no-load losses (r_t), the ratio of winding current to the rated value (r_i), the oil exponent (m), the average winding to average oil at the rated current (u), the hot spot factor (r_r), and the winding exponent (n). As seen in Eq. 16, both the ambient temperature (t_a) and the ocean surface temperature play a role in finding the operating temperature of the transformer. As the ocean surface water temperature fluctuates, the generated power of the OTEC plant and the current of the transformer windings change, which in turn affects the ratio of winding current to the rated value (r_i). In order to promptly assess the failure rate of the transformer for different air and ocean surface temperature, the Arrhenius law in Eq. 15 and the operating temperature of the transformer as Eq. 16 are used.

4.5 Cable

In order to effectively assess the failure rate of the XLPE cables used in the OTEC power plants, the operating temperature of them can be calculated as [19]:

$$t_c = t_a + r_1\left(r_e i^2 + \frac{dl}{2}\right) + nr_2(dl + r_e i^2(1+\alpha_1)) + n(r_3+r_4)(dl + r_e i^2(1+\alpha_1+\alpha_2)), \quad (17)$$

where the symbols r_1, r_2, r_3, r_4, α_1 and α_2 represent the thermal resistances and relative losses amongst the distinct layers of the cable, while r_e, i, dl and n stand for the electrical resistance of the cable conductor at the maximum operating temperature, the current flowing through the cable, the dielectric losses, and the number of conductors in the cable, respectively. The failure rate of the XLPE cable taking into account the fluctuations in ambient temperature and ocean surface temperature is calculated by utilizing the Arrhenius law as presented in Eq. 15 and the operating temperature of the XLPE cable calculated as Eq. 17. To determine the effect of temperature variation of the ocean surface water on the cable failure rate, the generated power of the OTEC plant considering the warm seawater temperature is calculated as (1). Then, the current of the cable is determined and by employing Eqs. 15 and 17, the cable failure rate is obtained.

5 Reliability assessment technique

In order to determine the reliability indices of the electric power distribution network containing close cycle OTEC power plants, it is crucial to consider the impact of temperature fluctuations on the generated power of the plants and the failure rates of its various components. The close cycle OTEC power plant is composed of several key elements which include the main structure, mooring system, pipes, pumps, turbine, evaporator, condenser, generator, transformer, and cable. The failure of any of these components results in the production capacity of the plant being reduced to zero. From a reliability perspective, these components can be considered to be in series and the equivalent failure and repair rates of the close cycle OTEC power plant are calculated as described in [52].

$$\lambda_{OTEC} = \sum_{k=1}^{n} \lambda_k \quad (18)$$

$$\mu_{OTEC} = \frac{\lambda_{OTEC}}{\sum_{k=1}^{n} \frac{\lambda_k}{\mu_k}} \quad (19)$$

The equivalent failure and repair rates of the OTEC power plant are represented by λ_{OTEC} and μ_{OTEC} respectively, while the failure and repair rates of the individual components that make up the power plant are represented by λ_k and μ_k. In order to perform an adequacy assessment of the power system containing a close cycle OTEC power plant and take into account the variable failure rates of its components, a procedure based on Monte Carlo simulation is proposed through the following 8 steps:

- Step 1. In this step, the hourly generated power of the understudied close cycle OTEC power plant is calculated based on the input data, including the hourly ocean surface temperature, the temperature of the deep seawater, and the characteristics of the plant, such as the mass flow rate of the working fluid, cold seawater, and warm seawater, the thermodynamic properties of the working fluid, and the efficiencies of the turbine and generator. The calculation is performed using Eqs. 1 to 11.
- Step 2: The hourly failure rates of the components of the OTEC power plant are calculated based on the reliability parameters of the components and utilizing Eqs. 12 to 17.
- Step 3. According to the Eqs. 18 and 19, the equivalent failure and repair rates of the understudied OTEC plant are determined.
- Step 4: The hourly unavailability and availability of the studied OTEC power plant and the other generation units in the power system are determined using Eq. 12.
- Step 5. At each hour, for the OTEC power plant and the other generation units of the understudied power system, random numbers are generated. In the generated number is in [0,A], the associated generation unit is up, and if the random number is in [A,1], the associated generation unit is down.
- Step 6. Based on the results obtained in the step 5, and the generated power of the OTEC power plant at the

associated hour, the total generation capacity of the power system at each hour is determined.

- Step 7. According to the hourly demand data, the total generation capacity of the power system is compared with the associated demand at each hour, and the value of the curtailed demand at each hour is determined.
- Step 7. The simulation approach is performed during a year including 8760 h to determine the yearly reliability indices such as the loss of load (demand) expectation (lole) in hours per year and the loss of energy expectation (loee) in MWh energy not supplied during a particular year.
- Step 8. The simulation is repeated for a duration of many years in order to determine the average values of the mentioned reliability indices as:

$$lole = \frac{\sum_{k=1}^{m\times 8760} b_k}{m} \tag{20}$$

$$loee = \frac{\sum_{k=1}^{m\times 8760} L_k}{m}, \tag{21}$$

where b_k is a binary number that is 1 when the demand at hour k is more than the total generation capacity of the power system, and is zero when the demand at the hour k is less than the generation capacity of the power system, L_k is the curtailed demand at hour k and m is the number of years that are simulated in the Monte Carlo simulation approach.

6 Numerical results

In this section, an assessment of the adequacy of the Roy Billinton Test System (RBTS) which includes a close cycle OTEC power plant is performed, with the aim of verifying the efficacy of the proposed method. The study focuses on a 30 MW close cycle OTEC power plant that employs ammonia as the working fluid. The temperature of the deep seawater sink is assumed to be 4 °C, and the hourly data regarding the ocean surface temperature associated to Hawaii in 2016 is presented in Fig. 5. The seawater temperature data is collected by thermistors located at a depth of about one meter [45]. Compared to other energy sources, the range of ocean surface temperature changes is quite low. As proven in [53], the amount of ocean surface temperature variation in a month is less than 2.5 °C. The amount of ocean surface temperature changes in most areas is less than the amount of changes occurred in the understudied region. The specifications of the understudied close cycle OTEC power plant are outlined in Table 1 [10, 11]. The failure rate of composed components should be obtained either from the components manufacturer or from the power plant operator. In this case, several years should have passed since the power plant enters into operation, and the operator of the power plant should regularly record the failure of parts. Due to the unavailability of this data, the values from studies [10, 11] have been used. In practice, turbine efficiency is dependent on the temperature of vapor passing through it. Besides, the performance of pumps such as efficiency and head depends on the temperature of fluids passing through them. For example, the efficiency of warm seawater pump is dependent on the ocean surface temperature. For the sake of simplicity, in the studied plant, the efficiency of the turbine is considered to be 1 and the efficiency of three applied pumps is considered to be constant and equal to 90%.

The assessment takes into account the failure rates of the variable of the components that make up the close cycle OTEC power plant. According to the location of installed OTEC plant, there are two types of plant including coastal or floating types. In this paper, the OTEC plant is considered to be installed on the coast. For coastal plants, the cold and

Table 1 Characteristics of the understudied OTEC power plant [10, 11]

Parameters	Value
Efficiency of turbine	1
Efficiency of three pumps	0.9
Generator efficiency	0.9
Ammonia mass flow rate	325 kg/s
Warm seawater mass flow rate	200 kg/s
Cold seawater mass flow rate	20 kg/s
Generator terminal voltage	1200 V
Main structure failure rate	0.5 occ./year
Main structure repair time	120 h
Warm seawater pump repair time	48 h
Turbine repair time	48 h
Generator repair time	48 h
Transformer repair time	72 h
Cable repair time	72 h
Mooring system failure rate	0.5 occ./year
Mooring system repair time	120 h
Pipes failure rate	0.5 occ./year
Pipes repair time	120 h
Evaporator failure rate	0.25 occ./year
Evaporator repair time	72 h
Condenser failure rate	0.25 occ./year
Condenser repair time	72 h
Working fluid pump failure rate	0.25 occ./year
Working fluid pump repair time	48 h
Cold seawater pump failure rate	0.25 occ./year
Cold seawater pump repair time	48 h
Control system failure rate	0.2 occ./year
Control system repair time	24 h

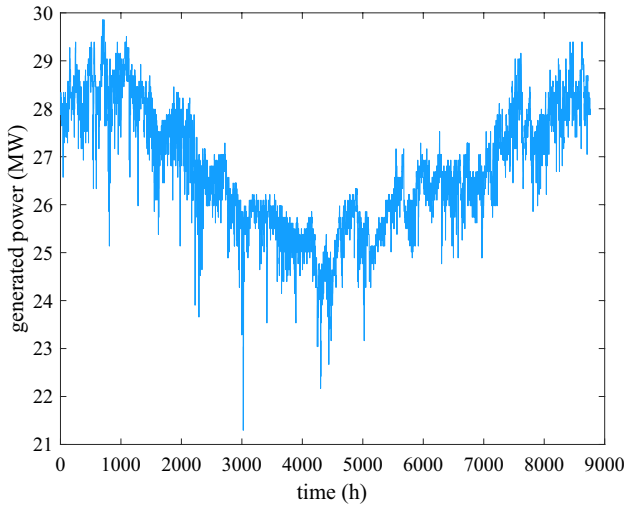

Fig. 7 Representation of the generated power of the understudied OTEC power plant

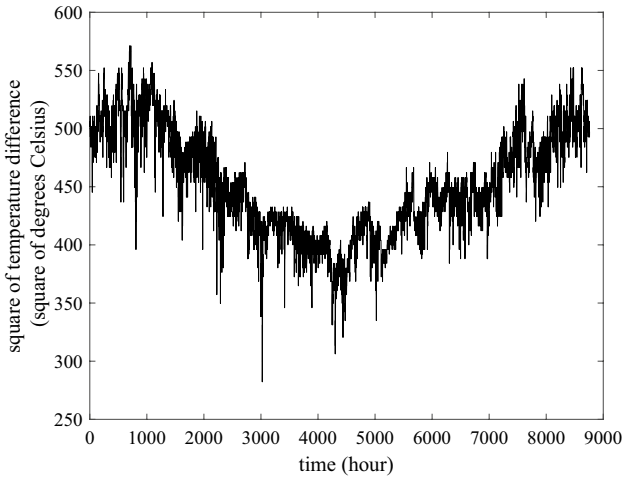

Fig. 8 Representation of square of temperature difference

warm seawater are transported to the power plant through pipes. The temperature of ocean surface and air temperature of the coast are different. Thus, depending on the location of warm seawater pumping, the temperature of surface seawater or seawater pumped from several-meters depth is used as temperature of warm seawater. For OTEC plants, such as Okinawa plant in Japan, that the surface seawater intake depth is 15 m or more, the temperature of warm seawater is less sensitive to air temperature than when the seawater is at several meters deep. Besides, for a floating OTEC plant, the surface seawater intake is below the bottom of the floating structure, so the surface seawater would be pumped from a seawater depth deeper than 15 m, and the warm seawater temperature has an inconsequential dependency on the air temperature. In the studied OTEC plant, to consider the variation of ocean surface temperature, it is assumed that the warm seawater is pumped from a 1-m ocean depth.

Based on the hourly ocean surface temperature and using the Eqs. 1 to 5, the hourly generated power of the understudied OTEC power plant is calculated and presented in Fig. 7. In general, the power produced by OTEC power plant is proportional to the square of the temperature difference between ocean surface and deep seawater. The hourly temperature difference between the ocean surface and deep seawater is computed and presented in Fig. 8. As it can be seen, the hourly power produced by studied PTEC plant illustrated in Fig. 7 is proportional to square of temperature difference between ocean surface and deep seawater presented in Fig. 8. In practice, the temperature of ammonia vapor is not same as surface seawater temperature. For determining the accurate temperature of ammonia vapor, the heat equation should be solved in the heat exchanger including warm seawater and ammonia. To determine the actual temperature of the ammonia, the amount of heat taken from the warm seawater is equal to the amount of heat needed to evaporate the ammonia. Besides, for determining the actual temperature of the ammonia leaving the condenser, the heat equation should be solved. Based on the amount of heat taken from the ammonia vapor and the heat given to the cold water in the heat exchanger, it is possible to obtain the temperature or the liquid ammonia. In [54] the actual temperatures of ammonia in the Rankine cycle of a real OTEC power plant are calculated. In more studies, for the sake of simplicity, the temperature of ammonia vapor and ammonia liquid are assumed to be the temperature of warm and cold seawater.

As mentioned in the third section, the temperatures of the seawater placed on the ocean surface and air affect the failure rates of some comprised elements of the OTEC power plant. In the studied OTEC power plant, the water of ocean surface and the seawater at a depth of 1000 m are pumped to the plant located on the coast. In this case, the devices, such as generator, transformer and cable, located in the plant are exposed to coastal air. As mentioned, these devices would normally be installed in a cool indoor location with a salt filter to avoid exposure to the coastal air. However, to study the impact of air temperature variation on the hazard rate of these components, it is assumed that they are installed outdoor. Thus, in addition to the seawater temperature, the hourly air temperature of the understudied site during a year is collected and presented in Fig. 9.

It is deduced from the third section, among different comprised components of the close cycle OTEC power plant, the variation in the temperature has no significant impact on the failure rate of the main structure, mooring system, pipes, cold seawater pump, working fluid pump and control system. However, the failure rates of the other elements comprising the close cycle OTEC power plant are affected

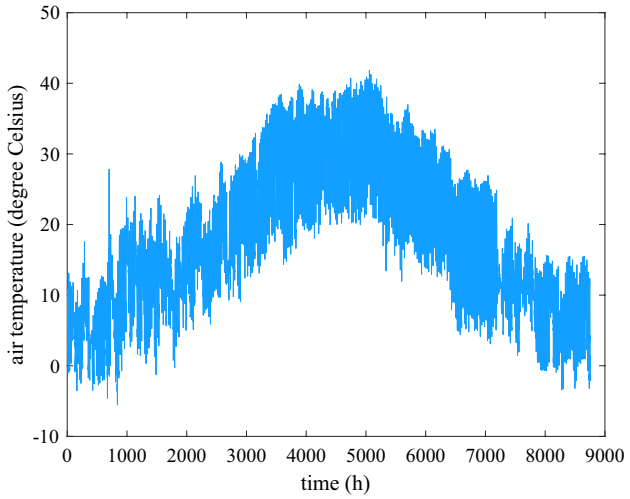

Fig. 9 Representation of the hourly air temperature during a year

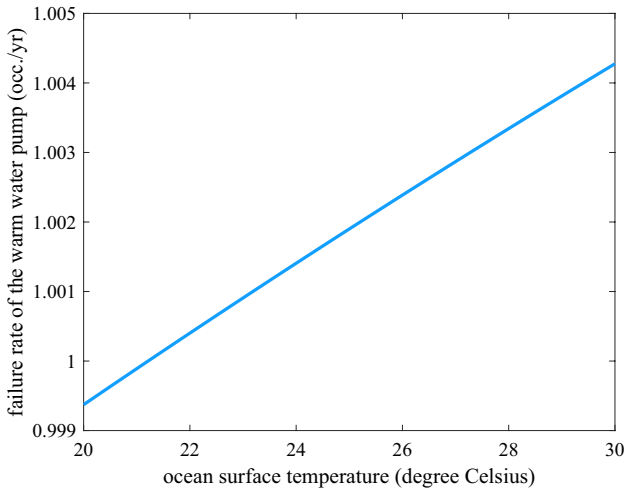

Fig. 10 The failure rate of the warm seawater pump versus the ocean surface temperature

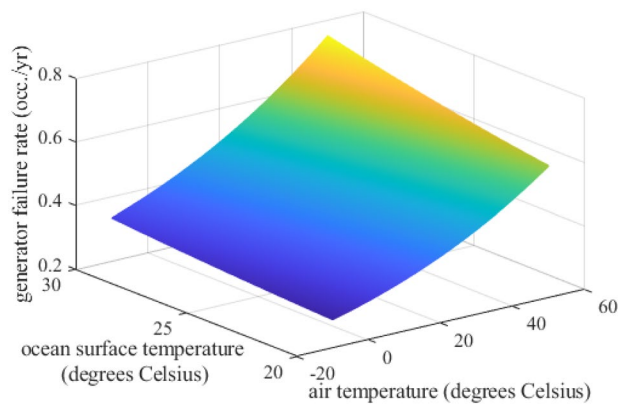

Fig. 11 The failure rate of the generator versus outside temperatures

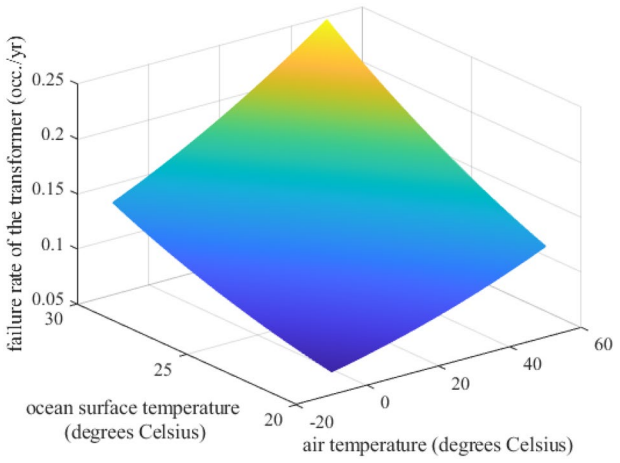

Fig. 12 The failure rate of the transformer versus outside temperatures

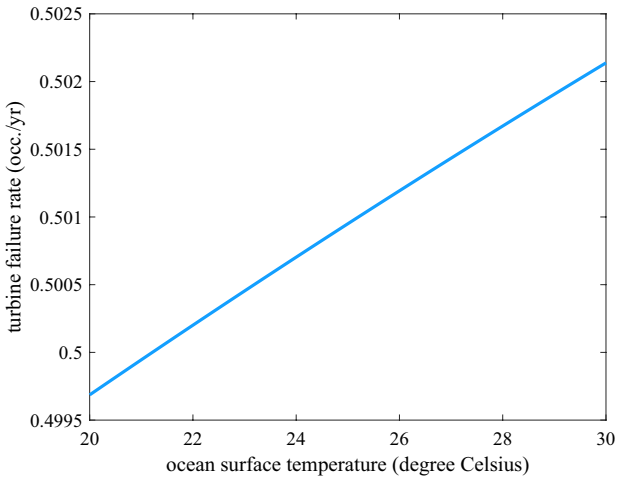

Fig. 13 The failure rate of the turbine versus the ocean surface temperature

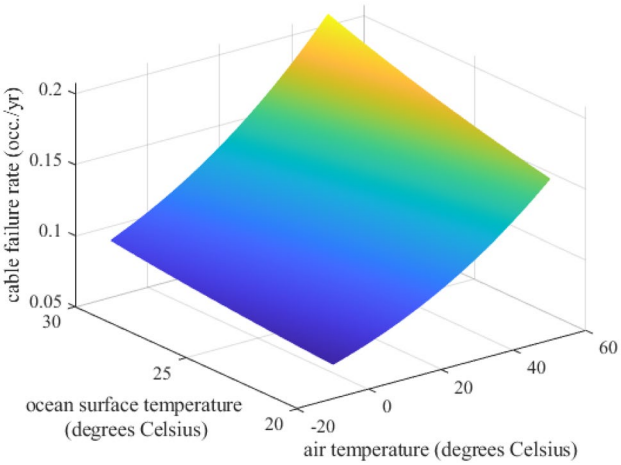

Fig. 14 The failure rate of the cable versus outside temperatures

by the variation in the temperature. According to the characteristics of the warm seawater pump, turbine, generator, transformer and cable [10–13], the failure rates of these components by taking into consideration the temperature variation are assessed by using the Eqs. 13 to 17, and presented in Figs. 10, 11, 12, 13 and 14.

As it can be seen in Figs. 10, 11, 12, 13 and 14, the failure rates of the warm seawater pump and turbine exhibit only a slight dependence on the ocean surface temperature. However, the other components of the close cycle OTEC power plant, including the cable, transformer, and generator, have a much more pronounced dependence on the temperatures of both the ocean surface and air. As a result, in the assessment of the power system that includes the close cycle OTEC power plants, it is necessary to take into account the variation in the failure rates of these components.

Except in special cases, generators, transformers, and cables are all installed indoors. If these appliances are placed outdoors, they are exposed to coastal salt damage, overheating and ultra violet degradation due to direct sunlight, which have a much higher risk of failure than air temperature. These devices, especially the transformer, can be placed in a temperature-controlled room. Besides, in the OTEC plant, a large amount of cold seawater is pumped to be used in air conditioning (cooling) system. Thus, the entire power plant, including the generator, transformer, and cable, can be kept at a lower temperature when compared with the outside temperature due to the influence of the cold seawater and working fluids that pass through the plant. In this situation, the air temperature has a negligible effect on the failure rate of this equipment. To determine the hazard rate of these components, the failure rate of them associated with room temperature is calculated. However, for studying the effect of temperature variation on hazard rate of these components, the worst case that may be the unrealistic assumption is addressed. In this study, it is assumed that the generator, transformer and cable are installed outdoors and are therefore exposed to the outside air temperature. Equation (18) is used to calculate the equivalent failure rate of the close cycle OTEC power plant, taking into consideration the fluctuations in the temperatures of both the ocean surface and air. This calculated equivalent failure rate is presented in Fig. 15 and it can be seen from the figure that the failure rate of the close cycle OTEC power plant varies in response to changes in the temperatures of the air and ocean surface water.

In this section, the hourly failure rate of the close cycle OTEC power plant under study is calculated and presented in Fig. 16. This calculation is performed by considering the hourly temperatures of the ocean surface water and air and the dependency of the equivalent failure rate of the OTEC plant on the temperature variations presented in Fig. 15. Utilizing this equivalent hourly failure rate of the plant, along with the equivalent repair rate calculated using Eq. 19, the

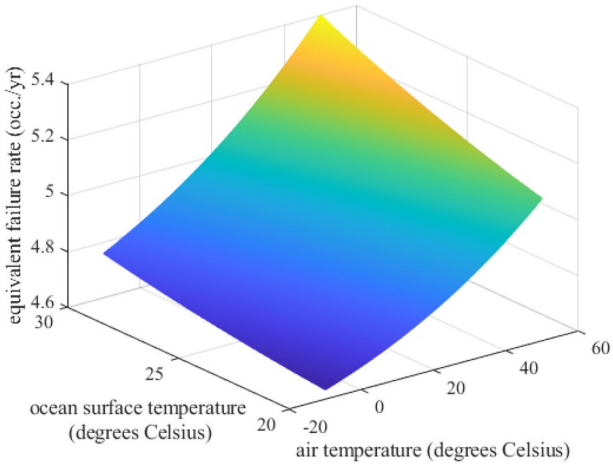

Fig. 15 The equivalent failure rate of the OTEC power plant versus outside temperatures

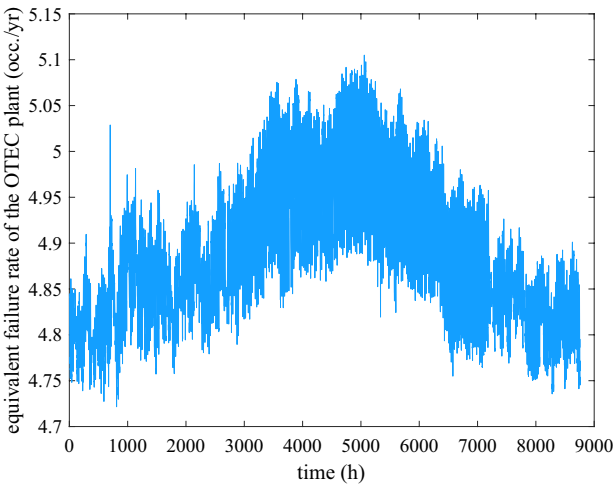

Fig. 16 The hourly equivalent failure rate of the OTEC power plant

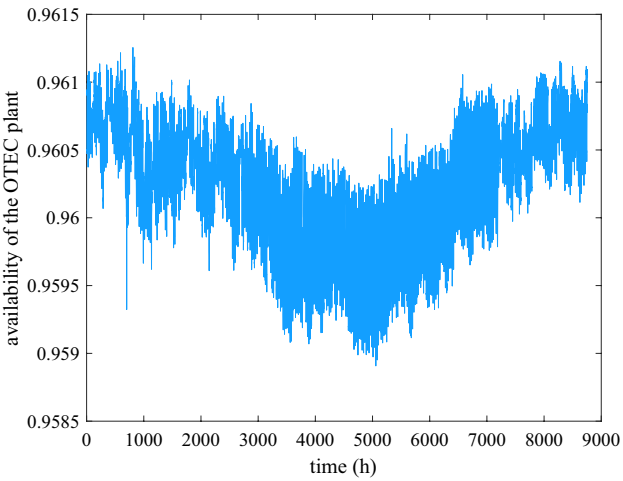

Fig. 17 The hourly availability of the OTEC power plant

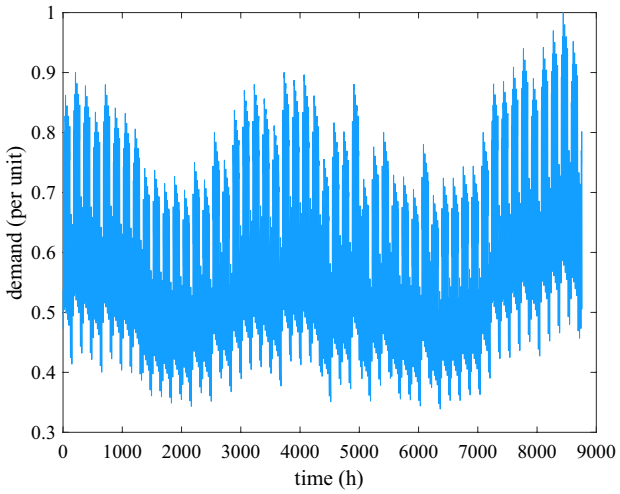

Fig. 18 The hourly demand of the system

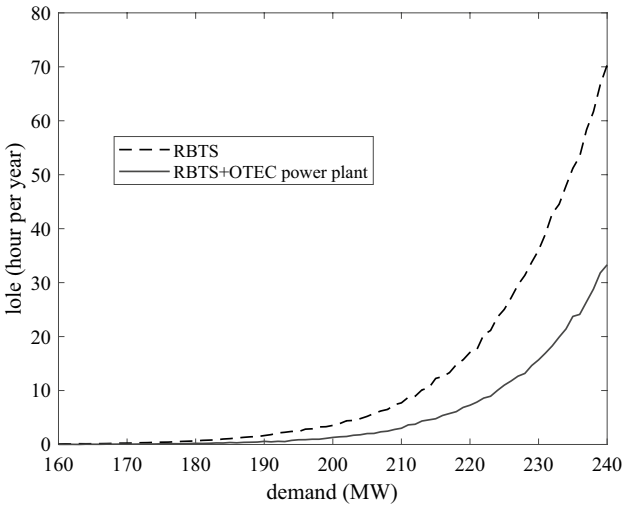

Fig. 19 Representation of the loss of load expectation versus demand

hourly availability of the OTEC plant is determined through Eq. 12 and presented in Fig. 17.

In this segment, the adequacy assessment of the RBTS comprising the studied OTEC power plant considering variable failure rate is performed. In this study, the net generated power of OTEC power plant is used to determine the reliability indices of the power system integrated with these renewable power plants. In [55], the generation capacities and reliability parameters of the generation units of the RBTS are provided. The hourly per unit demand of the system is considered to be based on the IEEE pattern that is presented in Fig. 18 [56]. In this study, the reliability indices of the understudied power system, including the loss of load expectation and the loss of energy expectation, are calculated and presented using the proposed Monte Carlo simulation-based technique and the availabilities of the RBTS and the hourly availabilities of the understudied close cycle OTEC power plant. The Monte Carlo method is repeated for 1000 years in order to achieve the desired accuracy. The results, depicted in Figs. 19 and 20, show that the reliability of the power system suffers a reduction as the demand rises. To enhance the reliability of the power system, the addition of a new generation unit, such as the understudied close cycle OTEC power plant, may be considered.

The adequacy indices calculated in the current paper are more accurate than the results obtained in [11], and this is due to:

- The impact of variation in seawater and air temperature on the failure rate of composed components of OTEC plant is not considered in [11], while, in this paper, hourly failure rate of composed components is calculated.
- The number of states in the reliability model of OTEC plant in [11] is decreased, and so, the accuracy of the reliability model decreases. While, in the current paper, by Monte Carlo simulation approach, the variation in the generated power of the OTEC plant at each hour is considered.
- In [11], for adequacy assessment of the power system containing OTEC plant, the load duration curve is considered, while, in the current paper, the variation of the demand in each hour is considered.

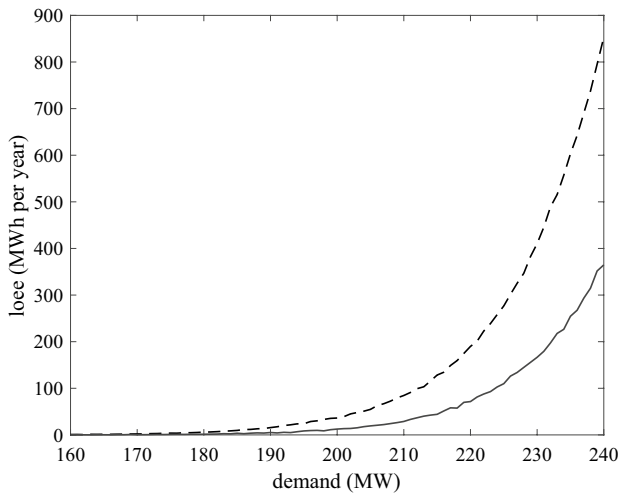

Fig. 20 The loss of energy expectation versus demand

7 Conclusion

In this study, a reliability assessment based on a Markov model of the OTEC systems considering temperature variation is proposed, one utilizing the method of Monte Carlo simulation. The purpose is to explore the intricacies of the power systems which include OTEC power plants. The variability of air and ocean surface temperatures have a profound effect on the generated power of the OTEC power plant, as well as the reliability of its various components such as the warm seawater pump, the turbine, the generator, the transformer, and the cable. To this end, we have sought to understand the dependence of these components on the temperatures of both air and ocean. Utilizing historical data from a site suitable for the installation of a large-scale OTEC power plant, we have calculated the hourly failure rates of each component, taking into account the hourly fluctuations in both seawater temperature and air temperature. It is evident that the ever-changing ocean and air temperatures have a significant impact on the failure rates of the primary elements of the OTEC power plant, a factor that must be considered when evaluating power system's adequacy that integrates these renewable resources. Using the variable failure rates of the components, we have calculated the adequacy indices of the power system, finding that the integration of OTEC power plants can indeed enhance the reliability performance of the power system. The results indicate that the failure rates of the warm seawater pump and turbine exhibit only a minimal correlation with the ocean surface temperature. In contrast, the components of the close cycle OTEC power plant, such as the cable, transformer, and generator, display a significant relationship with the temperatures of both the ocean surface and air. As seawater temperature increases, generator output also increases, which in turn affects the failure rate of generators, transformers, and cables. This highlights the need to consider the variation in the failure rates of these elements in the adequacy assessment of the power system that comprises OTEC power plants. This will be of great significance to those seeking to harness the power of the oceans in a responsible and sustainable manner.

Acknowledgements Radu Godina acknowledges Fundação para a Ciência e a Tecnologia (FCT-MCTES) for its financial support via the project UIDB/00667/2020 and UIDP/00667/2020 (UNIDEMI). Eduardo M. G. Rodrigues acknowledges Fundação para a Ciência e a Tecnologia (FCT-MCTES) for its financial support via the project UIDB/50021/2020 (INESC-ID).

Funding Open access funding provided by FCT|FCCN (b-on).

References

1. Rehman S, Alhems LM, Alam MdM, Wang L, Toor Z (2023) A review of energy extraction from wind and ocean: technologies, merits, efficiencies, and cost. Ocean Eng 267:113192. https://doi.org/10.1016/j.oceaneng.2022.113192
2. Cai L (2016) Performance evaluation and parametric optimum design of an updated ocean thermal energy conversion system. Ocean Eng 117:254–258. https://doi.org/10.1016/j.oceaneng.2016.03.026
3. Khan N, Kalair A, Abas N, Haider A (2017) Review of ocean tidal, wave and thermal energy technologies. Renew Sustain Energy Rev 72:590–604. https://doi.org/10.1016/j.rser.2017.01.079
4. Najafi A, Rezaee S, Torabi F (2011) Multi-objective optimization of ocean thermal energy conversion power plant via genetic algorithm. In: 2011 IEEE electrical power and energy conference, Winnipeg, MB, Canada, pp 41–46. https://doi.org/10.1109/EPEC.2011.6070237
5. Neill SP, Hashemi MR (2018) Fundamentals of ocean renewable energy: generating electricity from the sea. Academic Press, Cambridge
6. VanZwieten JH, Rauchenstein LT, Lee L (2017) An assessment of Florida's ocean thermal energy conversion (OTEC) resource. Renew Sustain Energy Rev 75:683–691. https://doi.org/10.1016/j.rser.2016.11.043
7. Etemadi A, Emdadi A, AsefAfshar O, Emami Y (2011) Electricity generation by the ocean thermal energy. Energy Procedia 12:936–943. https://doi.org/10.1016/j.egypro.2011.10.123
8. Arcuri N, Bruno R, Bevilacqua P (2015) LNG as cold heat source in OTEC systems. Ocean Eng 104:349–358. https://doi.org/10.1016/j.oceaneng.2015.05.030
9. Hopwood MW, Patel L, Gunda T (2022) Classification of photovoltaic failures with hidden markov modeling, an unsupervised statistical approach. Energies 15(14):14. https://doi.org/10.3390/en15145104
10. Ghaedi A, Nasiriani K, Nafar M (2020) Spinning reserve scheduling in a power system containing OTEC power plants. Int J Ind Electron Control Optim 3(3):379–391. https://doi.org/10.22111/ieco.2020.32602.1231
11. Nasiriani K, Ghaedi A, Nafar M (2022) Reliability evaluation for power systems containing ocean thermal energy conversion power plants. Sci Iran 29(4):1957–1974. https://doi.org/10.24200/sci.2020.54805.3927
12. Ghaedi A, Mirzadeh M (2020) The impact of tidal height variation on the reliability of barrage-type tidal power plants. Int Trans Electr Energy Syst 30(9):e12477. https://doi.org/10.1002/2050-7038.12477
13. Mirzadeh M, Simab M, Ghaedi A (2019) Adequacy studies of power systems with barrage-type tidal power plants. IET Renew Power Gener 13(14):2612–2622. https://doi.org/10.1049/iet-rpg.2018.5325
14. Mirzadeh M, Simab M, Ghaedi A (2020) Reliability evaluation of power systems containing tidal power plant. J Energy Manag Technol 4(2):28–38. https://doi.org/10.22109/jemt.2020.176501.1167

15. Ghaedi A, Gorginpour H (2021) Reliability-based operation studies of wave energy converters using modified PJM approach. Int Trans Electr Energy Syst 31(8):e12928. https://doi.org/10.1002/2050-7038.12928
16. Mirzadeh M, Simab M, Ghaedi A (2019) Reliability modeling of reservoir-based tidal power plants for determination of spinning reserve in renewable energy-based power systems. Electr Power Compon Syst 47(16–17):1534–1550. https://doi.org/10.1080/15325008.2019.1659453
17. Ghaedi A, Gorginpour H (2020) Reliability assessment of composite power systems containing sea wave slot-coned generators. IET Renew Power Gener 14(16):3172–3180. https://doi.org/10.1049/iet-rpg.2020.0572
18. Borges CLT (2012) An overview of reliability models and methods for distribution systems with renewable energy distributed generation. Renew Sustain Energy Rev 16(6):4008–4015. https://doi.org/10.1016/j.rser.2012.03.055
19. Leite da Silva AM, González-Fernández RA, Sales WS, Manso LAF (2010) Reliability assessment of time-dependent systems via quasi-sequential Monte Carlo simulation. In: 2010 IEEE 11th international conference on probabilistic methods applied to power systems, Singapore, pp 697–702. https://doi.org/10.1109/PMAPS.2010.5528326.
20. da Silva AML et al (2007) Application of Monte Carlo simulation to generating system well-being analysis considering renewable sources. Eur Trans Electr Power 17(4):387–400. https://doi.org/10.1002/etep.157
21. Khazraj H, da Silva FF, Bak CL, Hajibashi M (2018) Markov model of renewable resources for reliability assessment of distribution systems. In: 2018 IEEE international conference on environment and electrical engineering and 2018 IEEE industrial and commercial power systems Europe (EEEIC/I&CPS Europe), Palermo, Italy. pp 1–6. https://doi.org/10.1109/EEEIC.2018.8493814
22. Abdelsamad A, Lubkeman D (2019) Reliability analysis for a hybrid microgrid based on chronological Monte Carlo simulation with Markov switching modeling. In: 2019 IEEE power and energy society innovative smart grid technologies conference (ISGT), Washington, DC, USA. pp 1–5. https://doi.org/10.1109/ISGT.2019.8791611
23. Manco T, Testa A (2007) A Markovian approach to model power availability of a wind turbine. In: 2007 IEEE Lausanne Power Tech, Lausanne,Switzerland. pp 1256–1261. https://doi.org/10.1109/PCT.2007.4538496
24. Liu M, Li W, Wang C, Billinton R, Yu J (2016) Reliability evaluation of a tidal power generation system considering tidal current speeds. IEEE Trans Power Syst 31(4):3179–3188. https://doi.org/10.1109/TPWRS.2015.2473797
25. Liu M, Li W, Yu J, Ren Z, Xu R (2016) Reliability evaluation of tidal and wind power generation system with battery energy storage. J Mod Power Syst Clean Energy 4(4):636–647. https://doi.org/10.1007/s40565-016-0232-5
26. Ghaedi A, Gorginpour H (2021) Reliability evaluation of permanent magnet synchronous generator-based wind turbines considering wind speed variations. Wind Energy 24(11):1275–1293. https://doi.org/10.1002/we.2631
27. Ghasemi H, Shahrabi Farahani E, Fotuhi-Firuzabad M, Dehghanian P, Ghasemi A, Wang F (2023) Equipment failure rate in electric power distribution networks: an overview of concepts, estimation, and modeling methods. Eng Fail Anal 145:107034. https://doi.org/10.1016/j.engfailanal.2022.107034
28. Jiang K, Singh C (2011) New models and concepts for power system reliability evaluation including protection system failures. IEEE Trans Power Syst 26(4):1845–1855. https://doi.org/10.1109/TPWRS.2011.2156820
29. Ren Z et al (2018) Reliability evaluation of tidal current farm integrated generation systems considering wake effects. IEEE Access 6:52616–52624. https://doi.org/10.1109/ACCESS.2018.2866387
30. Li H, Guedes Soares C, Huang H-Z (2020) Reliability analysis of a floating offshore wind turbine using Bayesian networks. Ocean Eng 217:107827. https://doi.org/10.1016/j.oceaneng.2020.107827
31. Zio E (2013) The Monte Carlo simulation method for system reliability and risk analysis. Springer, London. https://doi.org/10.1007/978-1-4471-4588-2
32. Haghgoo O, Damchi Y (2022) Reliability modelling of capacitor voltage transformer using proposed Markov model. Electr Power Syst Res 202:107573. https://doi.org/10.1016/j.epsr.2021.107573
33. Najafi P, Talebi S (2021) Using real options model based on Monte-Carlo Least-Squares for economic appraisal of flexibility for electricity generation with VVER-1000 in developing countries. Sustain Energy Technol Assess 47:101508. https://doi.org/10.1016/j.seta.2021.101508
34. Raychaudhuri S (2008) Introduction to Monte Carlo simulation. In: 2008 winter simulation conference, Miami, FL, USA. pp 91–100. https://doi.org/10.1109/WSC.2008.4736059
35. Cevallos-Torres L, Botto-Tobar M (2019) Monte Carlo Simulation Method. In: Cevallos-Torres L, Botto-Tobar M (eds) Problem-based learning: a didactic strategy in the teaching of system simulation. Springer International Publishing, Cham, pp 87–96. https://doi.org/10.1007/978-3-030-13393-1_5
36. Goodarzi M et al (2022) Applying Bayesian Markov chain Monte Carlo (MCMC) modeling to predict the melting behavior of phase change materials. J Energy Storage 45:103570. https://doi.org/10.1016/j.est.2021.103570
37. Gupta G, Mishra RP, Jain P (2015) Reliability analysis and identification of critical components using Markov model. In: 2015 IEEE international conference on industrial engineering and engineering management (IEEM), Singapore. pp 777–781. https://doi.org/10.1109/IEEM.2015.7385753
38. Malinowski J (2021) 2—Markov modeling of multi-state systems with simultaneous component failures/repairs, using an extended concept of component importance. In: Pham H, Ram M (eds) Safety and reliability modeling and its applications. Elsevier, New York, pp 15–30. https://doi.org/10.1016/B978-0-12-823323-8.00018-0
39. Liang Q, Yang Y, Zhang H, Peng C, Lu J (2022) Analysis of simplification in Markov state-based models for reliability assessment of complex safety systems. Reliab Eng Syst Saf 221:108373. https://doi.org/10.1016/j.ress.2022.108373
40. Sinama F et al (2015) Thermodynamic analysis and optimization of a 10 MW OTEC Rankine cycle in Reunion Island with the equivalent Gibbs system method and generic optimization program GenOpt. Appl Ocean Res 53:54–66
41. Yoon J-I et al (2017) Analysis of the high-efficiency EP-OTEC cycle using R152a. Renew Energy 105:366–373
42. Yang M-H, Yeh R-H (2014) Analysis of optimization in an OTEC plant using organic Rankine cycle. Renew Energy 68:25–34. https://doi.org/10.1016/j.renene.2014.01.029
43. Li C, Pan L, Wang Y (2020) Thermodynamic optimization of Rankine cycle using CO_2-based binary zeotropic mixture for ocean thermal energy conversion. Appl Therm Eng 178:115617. https://doi.org/10.1016/j.applthermaleng.2020.115617
44. Wang M, Jing R, Zhang H, Meng C, Li N, Zhao Y (2018) An innovative Organic Rankine Cycle (ORC) based ocean thermal energy conversion (OTEC) system with performance simulation and multi-objective optimization. Appl Therm Eng 145:743–754. https://doi.org/10.1016/j.applthermaleng.2018.09.075
45. https://oceanservice.noaa.gov/. Accessed 1 Mar 2023
46. Li Z, Xu T, Gu J, Dong Q, Fu L (2018) Reliability modelling and analysis of a multi-state element based on a dynamic

Bayesian network. R Soc open sci 5(4):171438. https://doi.org/10.1098/rsos.171438
47. Billinton R, Allan RN (1992) Reliability evaluation of engineering systems: concepts and techniques, 2nd edn. Springer, New York
48. Budynas R, Nisbett K (2014) Shigley's mechanical engineering design, 10th edn. McGraw Hill, New York
49. Michel D (2018) Test of the formal basis of Arrhenius law with heat capacities. Phys A 510:188–199. https://doi.org/10.1016/j.physa.2018.06.125
50. Awadallah SKE, Milanović JV (2022) A probabilistic methodology for inclusion of transformer end-of-life failure in power system cascading failure simulations. In: 2022 17th international conference on probabilistic methods applied to power systems (PMAPS), Manchester,United Kingdom. pp 1–6. https://doi.org/10.1109/PMAPS53380.2022.9810587
51. IEC (2018) IEC 60076-7:2018 Power transformers—part 7: loading guide for oil-immersed power transformers. IEC: Geneva, Switzerland (2018). https://webstore.iec.ch/publication/34351, https://webstore.iec.ch/preview/info_iec60076-7%7Bed2.0%7Den.pdf
52. Billinton R, Allan RN (1988) Reliability assessment of large electric power systems, 1988th edn. Springer, Boston
53. Giostri A (2021) Off-design performance of closed OTEC cycles for power generation. Renew Energy 170:1353–1366
54. Engels W, Farshid Z (2014) Principle and preliminary calculation of ocean thermal energy conversion. ASEE 2014 Zone I conference, Bridgeport, USA
55. Billinton R et al (1989) A reliability test system for educational purposes-basic data. IEEE Power Eng Rev 9(8):67–68. https://doi.org/10.1109/MPER.1989.4310918
56. Grigg C et al (1999) The IEEE reliability test system-1996. A report prepared by the reliability test system task force of the application of probability methods subcommittee. IEEE Trans Power Syst 14(3):1010–1020. https://doi.org/10.1109/59.780914